Advances in ultrafast time resolved fluorescence physics for cancer detection in optical biopsy

R. R. Alfano[a]
Institute for Ultrafast Spectroscopy and Lasers, Departments of Physics and Electrical Engineering, The City College of the City University of New York, 160 Convent Avenue, New York, NY 10031, USA

(Received 30 August 2011; accepted 6 February 2012; published online 21 March 2012)

We discuss the use of time resolved fluorescence spectroscopy to extract fundamental kinetic information on molecular species in tissues. The temporal profiles reveal the lifetime and amplitudes associated with key active molecules distinguishing the local spectral environment of tissues. The femtosecond laser pulses at 310 nm excite the tissue. The emission profile at 340 nm from tryptophan is non-exponential due to the micro-environment. The slow and fast amplitudes and lifetimes of emission profiles reveal that cancer and normal states can be distinguished. Time resolved optical methods offer a new cancer diagnostic modality for the medical community. [http://dx.doi.org/10.1063/1.3697961]

I. INTRODUCTION

Optical spectroscopy is a novel approach for cancer detection and diagnosis in UV, visible and NIR parts of the spectrum. It has two main advantages over the conventional methods: 1) no tissue removal, and 2) *in situ* diagnosis in near real time. "Optical Biopsy" (OB), which encompasses optical physics and medicine has been known since it's first use in 1984 by Alfano.[1] The native fluorescence from malignant and nonmalignant breast and lung tissues were measured for the first time using spectra analysis.[1] OB is the only optical technique enabling the medical community to diagnose disease without removing tissue sample. It is suitable for margins assessment when extracting cancers *in situ* during surgery. Tissues contain a number of key fingerprint native endogenous fluorophore molecules: tryptophan, collagen, elastin, reduced nicotinamide adenine dinucleotide (NADH), flavin adenine dinucleotide (FAD) and porohyrins.[2–4] The absorption and emission spectra from key molecules in tissue are shown in Fig. 1.

"Optical biopsy" holds promise as clinical tool for diagnosing early stage of carcinomas and other diseases by combining with available photonic technology in particular endoscope and ultrafast streak camera technologies.

Fluorescence spectroscopy was used as a novel tool for detection of cancer in different tissue types in late 1980s on breast, lung, liver and GYN tissues.[1–3] The work was extended to differentiate human malignant breast tissues from benign and normal tissue-types using UV excitation.[2] OB technique can be used to extract intrinsic tissue fluorescence spectra during the induction of morphological and molecular changes in human tissue *in vivo*. Typical fluorescence spectra from ex vivo cancerous and normal breast tissue excited by 300 nm are shown in Fig. 2. Several groups have investigated various promising approaches using optical fluorescence with high sensitivity and specificity[1–12] and Stokes Shift spectroscopy[13–15] on different tissue types.

Time-resolved scattering and fluorescence spectroscopic measurements offer two optical physics approaches to extract the key fingerprint relaxation parameters and information of the fluorophores and scatterers in the medium and microenvironments of medium.[16,17] Theory of time-resolved

[a]Email: ralfano@ccny.cuny.edu

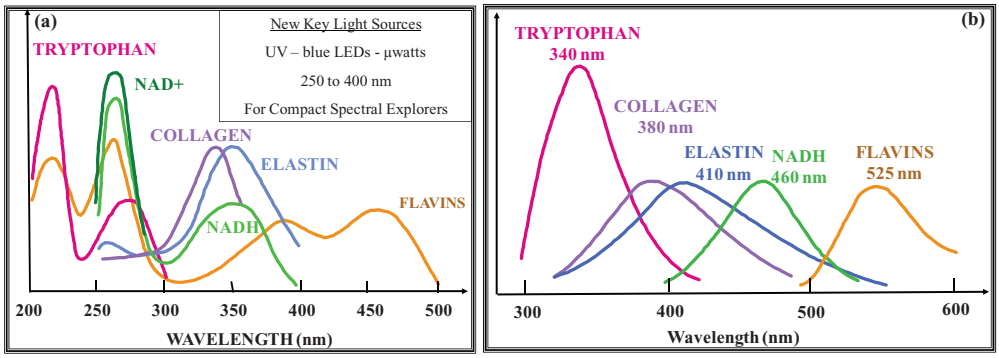

FIG. 1. (a) Absorption and (b) emission spectra of key fluorophores in human tissues: tryptophan, collagen, elastin, NADH and flavin.

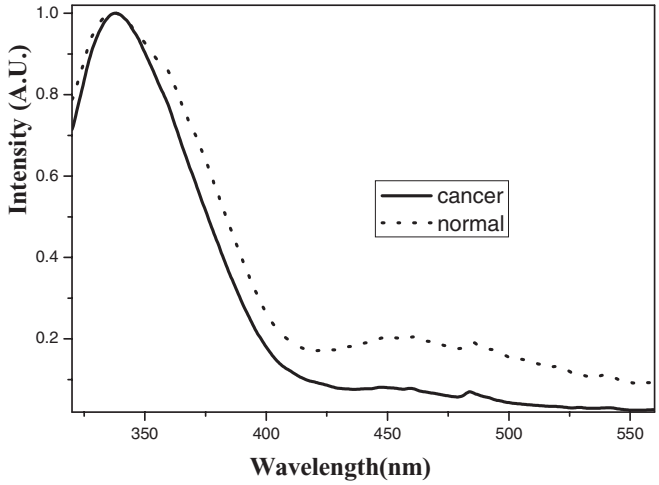

FIG. 2. Average fluorescence spectra of of cancerous (solid) and normal (dash) breast tissues obtained with the selective excitation wavelength of 300 nm.

fluorescence polarization kinetics of fluorohores in solution was highlighted by G. Weber[18] in nanosecond range and by G. R. Fleming in picosecond regime.[19] Alfano *et al.* demonstrated that fluorescence decay lifetimes from human breast cell lines[20] and rat kidney tissues[21] in the UV to NIR region and differentiated cancerous tissues from normal tissues.[22] The time-resolved fluorescence polarization dynamics was extended from solution to high scattering tissue medium and was systematically studied to investigate tissue microenvironment based on fundamentals of fluorophore rotational kinetics.[23,24]

Time resolved fluorescence measurements are lacking in the literature to obtain the key relaxation parameters: the nonradiative and radiative rates and quantum yield from different tissue types.

The objective of this paper is to summarize the basic fluorescence and demonstrate the usefulness of the time-resolved fluorescence spectroscopy techniques in medicine to obtain salient relaxation parameters of non radiative and radiative rates and distinguish the malignant and benign tumor tissues from normal tissues in various organs based on the differences of relaxation times and amplitude of optical signals at different emission and excitation wavelengths.

II. TIME-RESOLVED FLUORESCENCE PHYSICS MODEL

Time-resolved fluorescence studies can provide direct relaxation information on various underlying physical processes on a molecular and macromolecular scale. The basic theory[16] is used here to

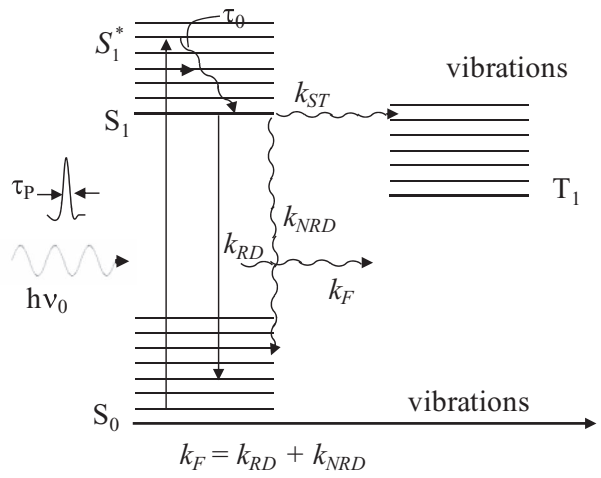

FIG. 3. Photo-physics processes in a simplified energy level diagram of a polyatomic organic molecule.

show how to extract the radiative and nonradiative from fluorescence dynamics. Direct picosecond time-resolved techniques under 100 fs laser excitation enable the study of dynamics of relaxation in macromolecules, particularly biopolymers such as proteins and nucleic acids using streak camera. Using time-resolved spectroscopic techniques, one may be able to isolate the participating fluorophores using wavelength selection of pump and emission using the supercontinuum fs and ps pulses.[25] This temporal analysis makes it possible to detect small changes in the environment of chromophores in the tissues. Besides studying molecular structure and underlying dynamics, the key parameters of fluorescence decay are determined and this can provide one with a new potential technique for medical diagnostic purposes.

In the biomedical area, Alfano and Yao[26] revitalized the use of light in dentistry by measuring the fluorescence lifetimes for decayed and non-decayed regions of calcified tissue. Extending this work, Alfano and his group found differences in fluorescence spectra and lifetimes from normal and malignant rat tissues[1] and later in human breast and lungs. They reported differences in fluorescence spectra and lifetimes from non-cancerous and cancerous tissues.[3,27]

The next section III demonstrates the potential use of spectral and temporal parameters for applications in cancer to unveil the underlying physics from the rate equation analysis given in reference 16. Femtosecond pulses provide δ(t) excitation to extract the risetime for the emission fluorescence. The photo-physics involved in the underlying dynamics first starts with an organic molecule being excited to S^*_n by an ultrashort delta δ(t) laser pulse in fs to ps range. The molecule relaxes from the excited state S^*_n, such as the vibrational excited state S^*_1 in figure 3, to the lowest level of the singlet state S_1 through vibrational relaxation at a rate of k_0, which gives vibrational thermalization time, $\tau_0 = k_0^{-1}$. The fluorescence rate is a measure of radiative and non-radiative processes. The constant k_R is the radiative decay rate (probability of radiative transition per second). Various other non-emission channels denoted as non-radiative decay processes are described by the rate k_{NR}. These non-radiative decay processes may occur due to collision by diffusion, quenching of emission by another species, energy transfer with fast rotational motion of the molecule, or transfer with diffusion while the molecule itself relaxes to the ground state. In general, if the molecular decay rates of internal conversion, intersystem crossing, and quenching are denoted as k_{IC}, k_{IS}, and k_q, respectively, then the non-radiative rate is given by

$$k_{NR} = k_{IC} + k_{IS} + k_q. \tag{1a}$$

The fluorescence decay rate is obtained from the radiative and non radiative rates given as:

$$k_F = k_R + k_{NR}, \tag{1b}$$

where the fluorescence lifetime $\tau_F = (k_F)^{-1}$.

The rate equation describing the dynamics of photo excited organic molecules in tissue with 100 fs δ(t) pulse excitation follows. The molecules excited into the first excited electronic –vibrational state S^*_1 are:

$$\frac{dn_{s_1^*}}{dt} = -k_0 n_{s_1^*} + n_0\delta(t). \tag{2}$$

Solving:

$$n_{s_1^*} = n_0 e^{-k_0 t}, \tag{3}$$

where n_0 is excited molecule of singlet S^*_1 at t = 0 and k_0 is vibrational relaxation rate. The rate of change of a number of molecules in the emitting state S_1 can be expressed as

$$\frac{dn_{s_1}}{dt} = k_0 n_{s_1^*} - k_F n_{s_1} \tag{4}$$

where n_{s_1} and $n_{s_1^*}$ are the number of molecules at the S_1 and S^*_1 (vibrational excited state of S_1) levels, respectively.

For a δ-pulse excitation, substituting for the number of molecules in the S^*_1 state as $n_{s_1^*} = n_0 e^{-k_0 t}$, one obtains

$$\frac{dn_{s_1}}{dt} = k_0 n_0 e^{-k_0 t} - k_F n_{s_1} \tag{5}$$

where n_0 is the number of molecules at S^*_1 at time $t = 0$. This equation can be further written as

$$\frac{d(n_{s_1} e^{k_F t})}{dt} = k_0 n_0 e^{(k_F - k_0)t}. \tag{6}$$

Integrating equation (6), one gets the population at S_1 at t:

$$n_{s_1}(t) = \frac{k_0 n_0}{k_0 - k_F}(e^{-k_F t} - e^{-k_0 t}) \tag{7}$$

The rise time gives the vibrational relaxation from S^*_1 of $\sim k_0^{-1}$ and the decay $\sim k_F$ gives the relaxation from S_1 to the ground state.

The fluorescence intensity at time t is proportional to n_{s_1} and can be expressed as

$$I(t) = k_R n_{S_1}(t) = k_R \frac{k_0 n_0}{k_0 - k_F}(e^{-k_F t} - e^{-k_0 t}) \tag{8}$$

The rise rate k_0 and decay rate k_F are obtained from measured I(t) vs time. The time to rise to the peak t_p gives a measure of rise and decay parameters. Taking the derivative dI/dt = 0, the rise time is given as

$$t_P = \ln(k_0/k_F)/(k_0 - k_F). \tag{9}$$

The size of fluorescence signal and the temporal profile give a measure of the quantum yield, Q:

$$Q = k_R/(k_R + k_{NR}) = k_R/k_F. \tag{10}$$

The yield:

$$Q = \frac{\tau_{NR}}{\tau_R + \tau_{NR}}. \tag{11}$$

For example, as a standard the parameters for Erythrosin dye in water are $Q = 0.02$ and τ_F = 68 ps. From Q and I(t) the values of τ_{NR}, τ_F, and τ_0 can be obtained to characterize materials.

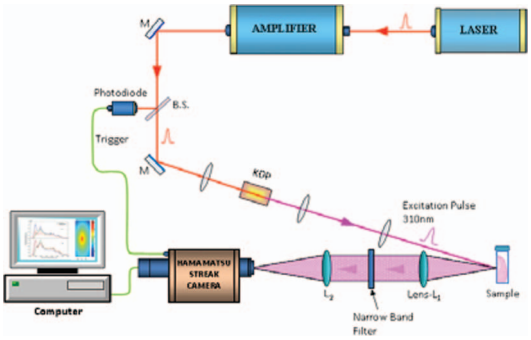

FIG. 4. Time-resolved fluorescence experimental set-up using a colliding pulse mode-locked dye laser-amplified-SHG laser system.

III. TIME-RESOLVED FLUORESCENCE STUDIES ON HUMAN BREAST TISSUES AT TWO DIFFERENT PUMP WAVELENGTHS OF 301 nm AND 353 nm

Steady-state ultraviolet (UV) fluorescence spectroscopy has been used to separate malignant tumors from benign and normal breast, cervical, ovarian, and uterus tissues and tumors. The tissue samples were excited at 300 nm using a lamp-based spectrometer and the emission was recorded from 320 nm to 550 nm as shown in figure 2. The ratios of fluorescence intensities at 340 nm to 440 nm for cancerous breast tissues were found to be different from that of normal and benign tissues.

In order to obtain further information on the chromophores responsible for the emission and to have a better physics picture of the heterogeneous nature of tissue fluorescence in cancerous and normal tissue, the kinetics of the physical processes occurring in tissues are studied using time-resolved fluorescence.

The key fluorescence relaxation decay parameters were determined from the time-resolved fluorescence spectroscopic data from photo-excited tissues. Non-malignant (normal, benign tissue, and benign tumor) and malignant breast tissues were excited at 310 nm and 353 nm. The measured fluorescence kinetics from malignant and non-malignant tissues exhibit different double exponential decay profiles consisting of slow and fast components.

A. Instrumentation

As an example, the schematic diagram of the time-resolved fluorescence experimental set-up is displayed in figure 4. Ultrafast 100 fs laser pulses (repetition rate, 82 MHz; $\lambda = 620 \pm 5$ nm; beam diameter, 3 mm) of 0.1 nJ per pulse were generated from a colliding pulse mode-locked dye laser system. These laser pulses were amplified by a sulphur rhodamine gain medium pumped by a copper vapour laser at 6.5 kHz. 100 fs laser pulses at 310 nm wavelength serve at $\delta(t)$ pulse were obtained by focusing the 620 nm beam onto a KDP crystal to generate the second harmonic. Breast tissue samples were put in quartz cells and excited at this wavelength. The pulse energy at the sample site was 0.5 μJ and the results were an average of a few tens of thousand pulses. The fluorescence was collected onto Hamamatsu synchroscan streak camera with a temporal resolution of 10 ps. The sampling volume was a fraction of 1 mm^2 in area and about a millimeter in depth. The tissue fluorescence was collected at the emission bands of 340±5 nm and 440±5 nm using narrowband filters to measure tryptophan, and collagen/elastin molecules in tissue. The resulting temporal profiles were fitted to double exponential impulse responses using nonlinear least-squares method. One can use Ti: sapphire laser and SHG to excite tissues at different wavelengths. The best choice for exciting biological materials for ultrafast physics studies is the Supercontinuum[25] from fibers, sapphire plates and solutions with wavelengths spanning from 400 nm to 2400 nm.

B. Materials and Methods

Time-resolved fluorescence measurements were performed on 18 samples from human breast of different subjects - six malignant tumors (all infiltrating ductal carcinomas; tumor cell differentiation was varied; nuclear grade was also varied), five benign tissues (fibrocystic mastopathy), five normal tissues (fibroglandular tissue and one lipoma) and two benign tumours (one fibroadenoma and one adenofibroma). Normal tissue refers to normal glandular tissue; benign tissue includes fibrosis–fibrous tissue; benign tumor includes fibroadenoma, which are neoplasms that usually do not recur after excision.

Most of samples were obtained from biopsies and were fresh, almost blood free, and not homogenized. They were obtained in chunks of about 5 mm × 5 mm × 5 mm in dimensions. The pathologist made the diagnosis of the tissue type.

C. Results

Typical time-resolved fluorescence profiles at 340 nm emission band from a benign breast tissue, a benign tumor and a malignant tumor, photoexcited at 100 fs 310 nm pulse, are displayed in Fig. 5. The temporal curves contain one slow and one fast component of fluorescence decay. The profiles for non-malignant (benign and normal) and malignant samples show a marked difference. The fast component seems to be more dominant in non-malignant tissues than in malignant tissues.

The fluorescence decay curves for 440 nm band appear to contain one slow and one fast component of fluorescence lifetime. Unlike the 340 nm band, there is no marked dominance of either component for 440 nm.

The time-resolved fluorescence profile is fitted to data by the expression

$$I(t) = a_s e^{-\frac{t}{\tau_s}} + a_f e^{-\frac{t}{\tau_f}} \tag{12}$$

The relaxation times and amplitudes of the fluorescence decay were obtained by a nonlinear least-squares fitting of the curves to the above expression. These measurements were performed at different points of the sample. It can be extended to a map of $\tau_F(r)$ over the tissue surface. The double exponential fit showed a chi-squared value close to 1, so that three or four component decay fits were not tested. Because of alignment problems only the amplitudes were compared. Two histograms of the amplitude ratios a_f/a_s and the slower decay time τ_s are given in figures 6 and 7, respectively. These histograms show the results for the 340 nm band which clearly distinguishes malignant from non-malignant tissue types. The data can be used to create a contour map of $\tau_F(r)$ on the surface of a tissue for separating diseased parts from normal region. Figures 6 and 7 plots are showing results separating cancerous and normal tissues using the time-resolved technique.

At the 340 nm band significant difference was found in the slow decay lifetimes of the malignant samples were found to be about twice as large as those in the case of non-malignant samples. The average τ_s for non-malignant and malignant tissues were 1.16 ± 0.28 and 1.91 ± 0.16 ns, respectively. The slower component was more dominant in malignant samples while the reverse was true in the case of non-malignant samples. The average ratios of amplitudes a_f/a_s for non-malignant and malignant tissues were 1.29 ± 0.51 and 0.39 ± 0.17, respectively. As the two histograms show, the relative amplitudes and the slower component of the fluorescence relaxation time can separate malignant breast tissues from non-malignant ones. There was consistency in the results from various positions of the non-malignant samples. However, the malignant samples did show variations towards non-malignant results at the peripheries when the sample was large. This was consistent with the pathologist's report of where the malignancy was located.

D. Discussion

From the results of the 340 nm band, a statistical study of these small number of samples was performed using a student '*t*' test. A '*p*' value of less than 0.001 was obtained between non-malignant and malignant results for τ_s and a_f/a_s. The '*p*' values were obtained separately for τ_s and a_f/a_s. These

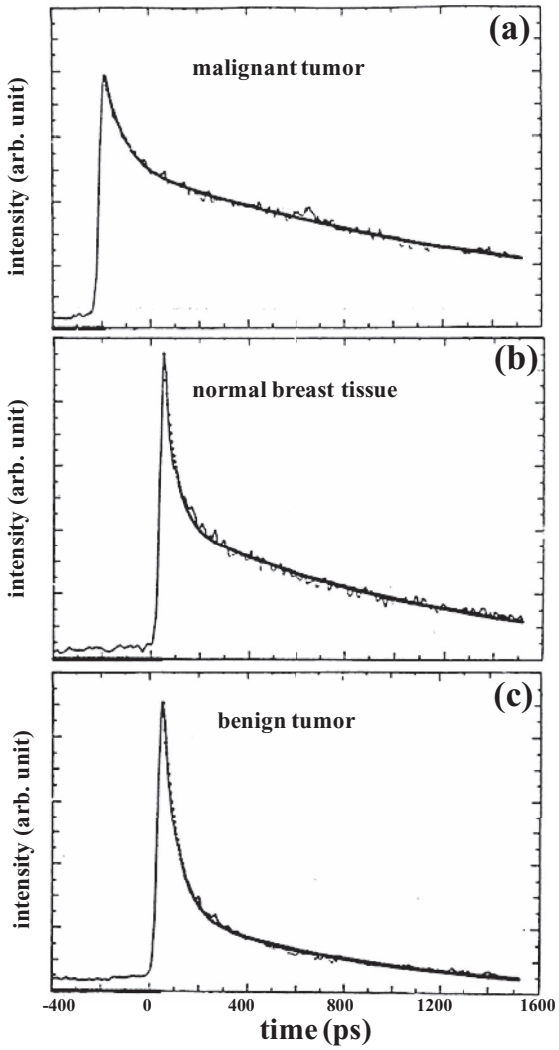

FIG. 5. Time-resolved fluorescence profiles with 310 nm excitation and 340 nm emission. (a) malignant tumor: $\tau_f = 79$ ps $\tau_s = 1.99$ ns, and $A_f/A_s = 0.5$; (b) normal breast tissue: $\tau_f = 46$ ps $\tau_s = 1.14$ ns, and $A_f/A_s = 1.2$; and (c) benign tumor: $\tau_f = 59$ ps $\tau_s = 0.89$ ns, and $A_f/A_s = 2.58$. All parameter were obtained by averaging.

results show how time-resolved fluorescence measurements can distinguish malignant tumors from non-malignant tissues.

At the 440 nm emission band no significant and consistent differences in lifetimes or amplitudes between malignant and non-malignant breast tissues were found arising from NADH, elastin and collagen.

The fluorescence yield at the 340 nm band, excited by 310 nm has been suggested to arise from tryptophan, or a combination of its residues. For λ_{ex} greater than 295 nm, fluorescence from tryptophan is more dominant than from tyrosine, both of which are present in most proteins. Tryptophan and its residues in different microenvironments have long been known to show double exponential fluorescence kinetics. The observation of double exponential fluorescence decays in tissues at 340 nm band with a fast component in the subnanosecond range and a slow component of about 1–2 ns suggests that the fluorescence could be from excited indole rings in tryptophan residues.

For 351 nm excitation, no remarkable results are observed from 450 nm emission, which is consistent with emission at 440 nm with 310 nm excitation.

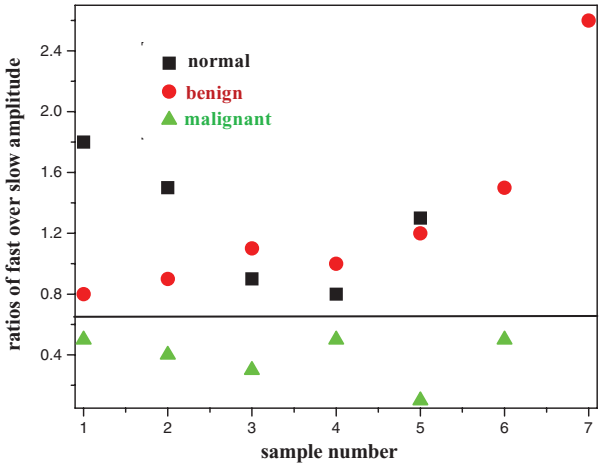

FIG. 6. The scatter plot of the amplitude ratios of A_f/A_s (initial intensity of fast component to slow component) for normal (square) breast tissue, benign (circle) and malignant (triangle) tumor.

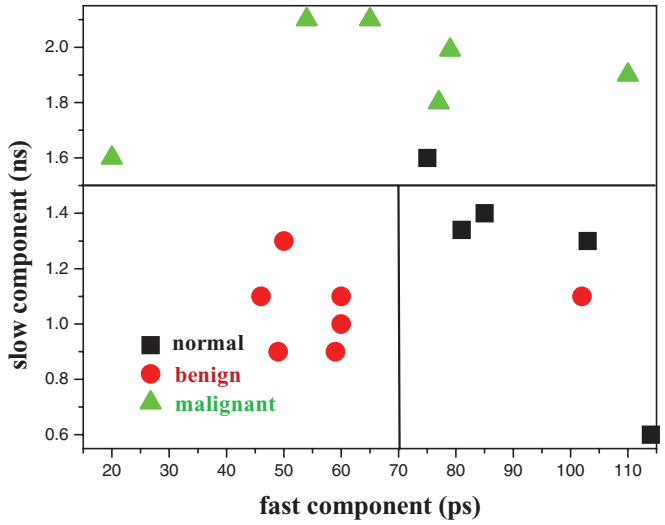

FIG. 7. The scatter plot of decay time (in nanosecond scale) vs. fast decay time (in picoseconds scale) of normal (square) breast tissue, benign (circle) and malignant (triangle) tumor.

The difference in fluorescence lifetimes and the dominance of one decay amplitude to the other in malignant and non-malignant tissues can be explained in two ways. One possibility could be the presence of two tryptophan residues in different proportions in cancerous and non-cancerous tissues. A second possibility could be due to different environments in the normal and abnormal tissues. Amplitudes and decay times of individual tryptophan conformers are strongly influenced by their microenvironments, such as different pH values and proximity of charged groups to the chromophores. Different pH values sometimes lead to charge transfers that give rise to an enhanced intramolecular interaction. This results in larger non-radiative energy losses. The dominance of the fast amplitude in the case of non-malignant samples could be due to more non-radiative processes occurring in the tryptophan residues of such tissues. The larger values of τ_s for malignant tissues suggest that more non-radiative processes occur in non-malignant tissue environments.

IV. SUMMARY

Time-resolved fluorescence spectroscopy method is reviewed using cancerous *ex vivo* tissue examples. The underlying physical and biological basis for cancer detection using optical approach was revealed using human breast, prostate, colon, gastrointestinal and gynecological samples. The results demonstrated that the emerging ultrafast time-resolved technique for optical biopsy in detection of cancer is promising for future clinical screening diagnosis and other important medical applications. An optical streak camera oscilloscope from Hamamatsu Corp. with optical fibers for excitation and detection would be ideal to scan and map a tissue in vivo, 80 ps time gated imager, such as a Picostar unit from LaVision can be used to obtain a 2D map of tissue.[28,29]

In conclusion, the outcome of this paper shows that the time resolved fluorescence is a novel way to obtain fundamental information on cancer.

ACKNOWLEDGMENTS

The research was support in part by DoD, ONR, DoE, NASA, the New York State Office Science - Technology and Academic Research (NYSTAR), and U. S. Army Medical Research and Material Command (USAMRMC). The author acknowledges the help of NDRI and CHTN for providing normal and cancer tissue samples for the measurements. He acknowledges the contributions over the years from the researchers at IUSL at CCNY: Mrs. C.-H. Liu, Dr. S. S. Lubicz (M.D.), Prof. Y. L. Yang, Dr. W. B. Wang, Mr. G. C. Tang, Ms. A. Alimova, Mr. Y. Budansky, Dr. A. Pradhan, Dr. B. B. Das, as well as Dr. S. P. Schantz (M.D.) and Dr. H. E. Savage from Manhattan Eye, Ear & Throat Hospital and Memorial Sloan Kettering Cancer Center (MSKCC), Dr. Joseph Cleary (M.D.), NY Medical, D. Vitenson (M.D.), Hackensack Medical Center, and Dr. Jason A. Koutcher (M.D.) from Memorial Sloan Kettering Cancer Center (MSKCC). Special thanks goes to Dr. Yang Pu and Dr. K. Sutkus in helping with writing this manuscript.

[1] R. R. Alfano, D. Tata, J. Cordero, P. Tomashefsky, F. Longo and M. Alfano, "Laser induced fluorescence spectroscopy from native cancerous and normal tissue," IEEE J. Quantum Electron., **20**, 1507-1511 (1984).
[2] R. R. Alfano, B. B. Das, J. B. Cleary, R. Prudente and E. Celmer, "Light sheds light on cancer," Bull. NY Acad. Med., **67**, 143-150 (1991).
[3] R. R. Alfano, G. C. Tang, Asima Pradhan, W. Lam, Daniel S. J. Choy, Elana Opher, "Fluorescence Spectra from Cancerous and Normal Human Breast and Lung Tissues," IEEE J. of Quant. Electron QE, **23**, 1806 (1987).
[4] G. M. Palmer, P. J. Keely, T. M. Breslin and N. Ramanujam, "Autofluorescence spectroscopy of normal and malignant human breast cell lines," Photochem.& Photobiol., **78**(5), 462–469 (2003).
[5] M. B. Silberberg, H. E. Savage, P. G. Sacks, S. P. Schantz, G. C. Tang and R. R. Alfano, "Detecting retinoic acid-induced biochemical alterations in squamous cell carcinoma using intrinsic fluorescence spectroscopy," The Laryngoscope, **104**(3), 278–282 (1994).
[6] Y. Pu, W. B. Wang, G. C. Tang and R. R. Alfano, "Changes of collagen and NADH in human cancerous and normal prostate tissues studied using fluorescence spectroscopy with selective excitation wavelength," J. Biomed. Opt., **15**, 047008-1-5 (2010).
[7] J. J. Baraga, R. P. Rava, P. Taroni, C. Kittrell, M. Fitzmaurice, M. S. Feld, "Laser induced fluorescence spectroscopy of normal and atherosclerotic human aorta using 306–310 nm excitation," Lasers Surg. Med., **10**, 245–61 (1990).
[8] B. Lin, S. Urayama, R. Saroufeem, D. Matthews and S. G. Demos, "Real-Time Microscopic Imaging of Esophageal Epithelial Disease with Autofluorescence under Ultraviolet Excitation," Opt. Express, **17**(15), (2009).
[9] I. J. Bigio and J. R. Mourant, "Ultraviolet and visible spectroscopies for tissue diagnosis," Phys Med Biol, **42**, 803–14 (1997).
[10] R. Drezek, K. Sokolov, U. Utzinger, I. Boiko, A. Malpica, M. Follen and R. Richards-Kortum, "Understanding the contributions of NADH and collagen to cervical tissue fluorescence spectra: Modeling, measurements, and implications," J. Biomed. Opt., **6**(4), 385–396 (2001).
[11] M. Panjehpour, C. E. Julius, M. N. Phan, T. Vo-Dinh, S. Overholt, "Laser-induced fluorescence spectroscopy for *in vivo* diagnosis of non-melanoma skin cancers," Lasers Surg. Med., **31**, 367—373 (2002).
[12] I. Georgakoudi, B. C. Jacobson, M. G. Muller, E. E. Sheets, K. Badizadegan, D. L. Carr-Locke, C. P. Crum, C. W. Boone, R. R. Dasari, J. V. Dam and M. S. Feld, "NAD(P)H and collagen as *in Vivo* quantitative fluorescent biomarkers of epithelial precancerous changes," Cancer Res., **62**, 682–687 (2002).
[13] R. R. Alfano and Y. Yang, "Stokes shift emission spectroscopy of human tissue and key biomolecules," IEEE J. Quantum Electron., **9**(2), 148-153 (2003).
[14] R. R. Alfano, Y. Yang, "Stokes Shift Emission Spectroscopy for Detection of Disease and Physiological State of Specimen," U.S.A. patent #7,192,783, March 20, (2007).

[15] J. Ebenezar, Y. Pu, C. H. Liu, W. B. Wang, and R. R. Alfano, "Diagnostic Potential of Stokes Shift Spectroscopy of Breast and Prostate Tissues - A preliminary pilot study," Technol. Cancer Res. Treat. **10**, 153-161 (2011).
[16] B. B. Das, F. Liu, and R. R. Alfano, "Time-resolved fluorescence and photon migration studies in biomedical and model random media," Rep. Prog. Phys., **60**, 227–292 (1997).
[17] Y. Pu, W. B. Wang, B. B. Das, and R. R. Alfano, "Differences of Time-resolved near infrared spectral wing emission and imaging of human cancerous and normal prostate tissues," Opt. Commun., **282**, 4308–4314 (2009).
[18] R. D. Spencer and G. Weber, "Influence of Brownian rotations and energy transfer upon the measurements of fluorescence lifetime," J. Chem. Phys. **52**, 1654-1663 (1970).
[19] G. R. Fleming, J. M. Morris and G. W. Robinson, "Direct observation of rotational diffusion by pico-second spectroscopy," Chemical Physics, **17**, 91-100 (1976).
[20] W. S. Glassman, M. Steinberg and R. R. Alfano, "Time-resolved and steady state fluorescence spectroscopy from normal and malignant cultured human breast cell lines," Lasers in Life Sci., **6**, 91–98 (1994).
[21] D. B. Tata, M. Foresti, J. Cordero, P. Tomashefsky, M. A. Alfano and R. R. Alfano, "Fluorescence polarization spectroscopy and time-resolved fluorescence kinetics of native cancerous and normal rat kidney tissues," Biophys. J., **50**, 463-469 (1986).
[22] A. Pradhan, B. B. Das, K. M. Yoo, J. Cleary, R. Prudente, E. Celmer, and R. R. Alfano, "Time-resolved UV photoexcited fluorescence kinetics from malignant and non-malignant breast tissues," Lasers in Life Sci., **4**(4), 225-234 (1992).
[23] Y. Pu, W. B. Wang, S. Achilefu and R. R. Alfano, "Study of rotational dynamics of receptor-targeted contrast agents in cancerous and normal prostate tissues using time-resolved picosecond emission spectroscopy," Appl. Opt., **50**, No. 7, 1312-1322 (2011).
[24] S. G. Demos, H. Savage, A. S. Heerdt, S. Schantz, R. R. Alfano, "Time-resolved degree of polarization for human breast tissue," Opt. Commun. **124**, 439-442 (1996).
[25] R. R. Alfano and S. L. Shapiro, Observation of Self-Phase Modulation and Small Scale Filaments in Crystals and Glasses, Phys. Rev. Lett. **24**, 592-594 (1970); R. R. Alfano, *The Supercontinuum Laser Source*, Springer Verlag, New York (1989).
[26] R. R. Alfano, and S. S. Yao, "Human teeth with and without dental caries studied by visible luminescent spectroscopy," J Dent Res., **60**(2), 120–122 (1981).
[27] R. R. Alfano, G. C. Tang, A. Pradhan, M. Bleich, D. S. J. Choy and E. Opher, "Steady State and Time-Resolved Laser Fluorescence from Normal and Tumor Lung and Breast Tissues," J. of Tumor Marker Oncology, **3**, 165 (1988).
[28] R. R. Alfano, Picosecond gated light detector tube, US patent No. 4,682,020; Ultrafast gated light detection, US patent No. 4,659,921, April 21, 1987.
[29] R. R. Alfano and N Schiller, Compact Temporal Spectral Photometer, US patent No. 4,630,925, December 23, 1986.